Arabian Journal for Science and Engineering (2020) 45:8999–9014
https://doi.org/10.1007/s13369-020-04649-6

RESEARCH ARTICLE-MECHANICAL ENGINEERING

Investigation on Drilling Behavior of CFRP Composites Using Optimization Technique

D. Raj Kumar[1] · N. Jeyaprakash[2] · Che-Hua Yang[2,3] · K. R. Ramkumar[4]

Received: 29 August 2019 / Accepted: 17 May 2020 / Published online: 1 June 2020

Abstract

Carbon fiber-reinforced polymers (CFRPs) have been applied to various fields such as electronic printed circuit boards, aircraft brakes, automobile forks, and machine tool-damped structures due to their low density and high tensile strength. These application components required micro-hole and macro-hole in it for joining. In this research work, a comparison of the experimental investigation on micro- and macro-drill on CFRP using a vertical machining center has been carried out. The input machining control factors were spindle speed and rate of feed, whereas the quality characteristics of drilling CFRP were considered as thrust force, delamination, and overcut. Analysis of variance (ANOVA) and gray relational analysis were employed to identify the most significant factor and optimum process parameters, respectively. Microstructural defects of micro-hole and macro-hole were studied using scanning electron microscopy. Results showed that the rate of feed linearly affected the thrust force and delamination and is inversely proportional to overcut.

Keywords CFRP · Micro- and macro-drill · Thrust force · Delamination · Overcut · Optimization

1 Introduction

Compared to the various fiber-reinforced composites, the adaptability of carbon fiber-reinforced polymer (CFRP) in various fields like electronic industries fabricating the printed circuit boards, aircraft brakes, automobile forks, and machine tools-damped structure is increased because of its properties such as low density and high tensile strength [1]. The CFRP material is applied for various parts such as PCBs, satellite antenna, wheelchairs, computer body panels, and these components need micro- and macro-drill in it. Therefore, micro-drilling and macro-drilling on CFRP material have been attempted in this work. The micro-hole and macro-hole making process on CFRP can be performed by employing mechanical drilling, laser drilling, and abrasive water jet machining. In mechanical drilling, the CFRPs have various defects on machined surface such as fiber pullout, delamination, fuzzing, spalling, and fiber breakout due to the nature of material properties, improper selection of drilling condition, tool geometry, and tool materials [2]. Similarly, problems in laser drilling are thermal damage (both fiber and matrix), taper angle, and heat-affected zone in the cut surface because of thermal effects on the selection of process conditions. The problems in abrasive water jet machining are jet-lag, kerf taper angle, and surface roughness because of lack of information in an inadequate selection of condition and carbon fiber absorbs water [3]. The measurement of micron-level features is also a difficult task because of the inadequate development of micrometeorology. The X-ray, ultrasonic C-scan, optical microscope, and digital photograph are commonly used to find the delamination. The delamination is a major problem in CFRP composite,

✉ N. Jeyaprakash
prakash84gct@gmail.com; prakash@ntut.edu.tw

D. Raj Kumar
profdrajkumar@gmail.com

Che-Hua Yang
chyang@ntut.edu.tw

K. R. Ramkumar
get2raam@gmail.com

[1] Department of Mechanical Engineering, MAM School of Engineering, Tiruchirappalli, India

[2] Additive Manufacturing Center for Mass Customization Production, National Taipei University of Technology, Taipei 10608, Taiwan, ROC

[3] Institute of Manufacturing Technology, National Taipei University of Technology, Taipei 10608, Taiwan, ROC

[4] Department of Metallurgical and Materials Engineering, Indian Institute of Technology Madras, Chennai, India

and its rejection rate is 60%. Hence, the selection of proper process parameters is necessary for the drilling process. It was revealed that adequate information on the machine tool is required for the processing of the CFRP composites [4]. In conventional CFRP machining, the higher hole surface quality was obtained by increasing spindle speed and decreasing the rate of feed. Also, it was found that the minimum delamination factor was obtained by reducing the cutting force and feed rate [5]. The delamination was achieved in the range of 12.8–25.7% on the CFRP micro-hole by adopting the rotary ultrasonic helical machining [6]. In another way, by changing the tool geometry, tool types, providing backup plate and high-speed drilling, the delamination of CFRP was reduced [7]. Also, the laminate orientation and workpiece constituents of CFRP were also related to delamination on CFRP [8]. The cryo-treated WC drill produced better delamination than untreated drill [9]. Besides, the chilled air environment produced a better delamination factor compared to dry air [10]. The circular drilling strategy decreased the delamination factor compared to grinding [11]. The performance of high-speed steel, tipped carbide, and solid carbide drill on CFRP was evaluated based on the thrust force and torque. The result found that the solid carbide drill produced better performance over other drills [12]. Therefore, various strategies were followed by many researchers to improve the hole quality. The selection of cutting conditions for the machining of CFRP was important to work smoothly without defects. Because of the processing of CFRP composite, drilling variables such as drill velocity and drill feed were greatly influencing delamination, thrust force, and an overcut. It was revealed that the minimum delamination was achieved by increasing the spindle speed and lowering the rate of feed. The quality of the drilled hole in CFRP composite was better by using the spindle speed ranges from 800 to 3000 rpm and feed rate ranges from 100 to 1000 mm/min [13]. The drilling of CFRP laminates using twist drills found that enlargement of drill diameter increased the thrust force. Drilling trials were performed on CFRP laminates using different twist drills. It was found that the diameter of the drill contributes to the improvement in overall machining performance and recognized as the most predominantly influencing factor which affects the delamination and thrust force. Drilling experiment was performed on CFRP/Al stacks using carbide drills in various drill sizes. It was observed that there was an increase in thrust force during drill with lesser diameter than larger diameter of drill bits [14]. Drilling on carbon fiber-reinforced polypropylene composite resulted that a feed rate mainly affected the thrust force and torque [15]. Investigations made on drilling characteristics of CFRP composite found that there was a remarkable increase in the thrust force as the diameter of drill increased. It was suggested that smaller diameter drills reduced the thrust force during drilling process.

From the above literature, it is clear that the influences of micro-drill parameters have studied metals and composites. However, there is no literature on the comparison of micro- and macro-drill process parameters on CFRP using Taguchi-based gray relational analysis. As drilling operation becomes more extensive in the industry, the research and development of these applications in the field of aerospace, electronic, and automobile have changed their attention to improving the drilling quality. The comparison of two various drill (micro and macro) has given a better understanding in terms of delamination, thrust force, and overcut. In the present study, experimental investigation has been proposed for analyzing the micro-hole and macro-hole quality on CFRP using vertical machining center (VMC). The relations between thrust force, delamination, and overcut for various drill diameters have been analyzed. Taguchi's experimental approach has been followed to minimize the experiment trails, and L_9 orthogonal array has been used to perform the experimental runs. Besides, ANOVA has been performed to find out the significance of process variables. Optimum levels were found using gray relational analysis (GRA), and roughness of machined hole has been analyzed.

2 Materials and Methods

The CFRP sample in the form of the plate by having the dimensions of $100 \times 60 \times 3$ mm was used in the present study. The CFRP sample which is considered for the present study has 55% of carbon fibers; epoxy matrix, 12 layers; 0° and 90° of fiber orientation. This composite was designed and fabricated using the autoclave method. The model picture of CFRP plate with dimensions, SEM images of CFRP plate [16], and schematic representation of CFRP plate with fiber orientation is shown in Fig. 1a–c. The HARDINGE VMC 800II was used for conducting the experiments. The considered input variables for this investigation are spindle speed and rate of feed. Two factors and three levels were used to run the experiments. The process conditions were selected based on the available literature and present trail test. The selected process variables and levels are shown in Table 1. The schematic diagram of the experimental setup is shown in Fig. 2. The micro- and macro-drill geometrical dimensions have been measured using an optical microscope as shown in Fig. 3, and the details are presented in Table 2. Table 3 exhibits the measurement of performance characteristics. Before the drilling process, drill collet with micro-drill bit has been fixed in main spindle drive and work material is fixed on digital strain gauge dynamometer. The machining experiments have been performed under dry conditions. During drilling, thrust force (F_y) for each trial has been measured using a digital strain

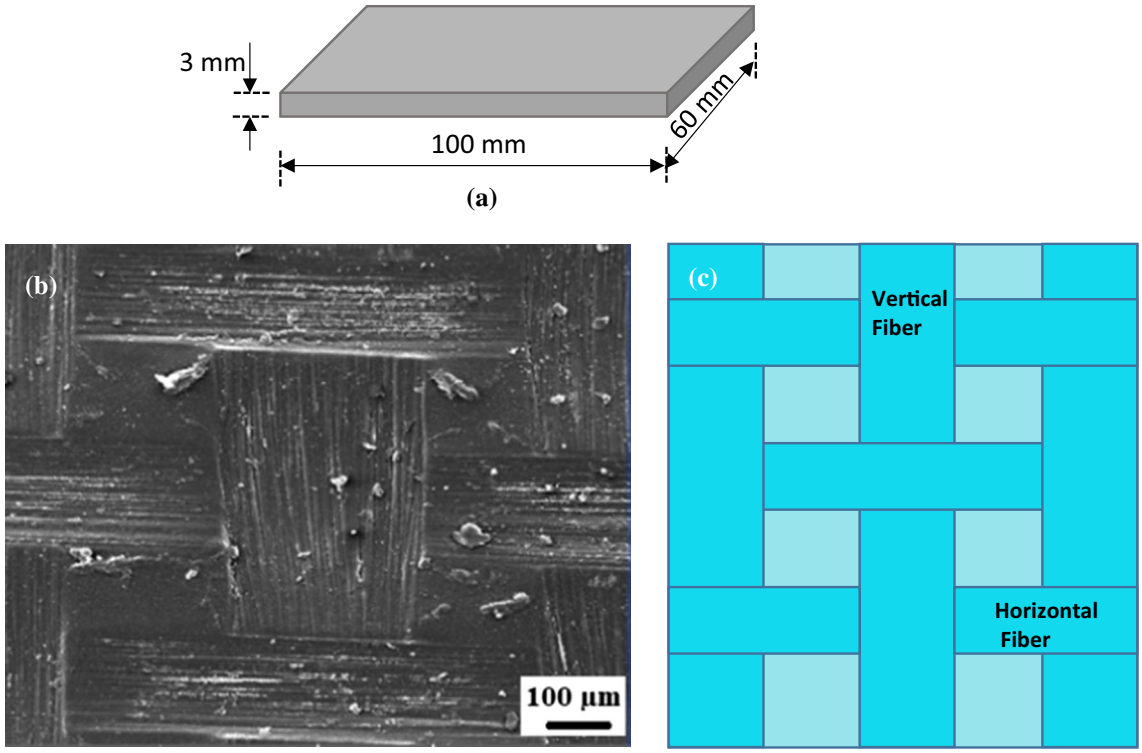

Fig. 1 Model picture of CFRP plate with dimensions (**a**), SEM images of CFRP plate (**b**) [16], schematic representation of CFRP plate with fiber orientation (**c**)

Table 1 Levels and parameters

Parameters	Levels		
	1	2	3
Spindle speed (*V*) (rpm)	2000	2500	3000
Rate of feed (*F*) (mm/rev)	0.01	0.03	0.05
Micro-drill diameter (mm)	0.3	0.4	0.5
Macro-drill diameter (mm)	1	2	3

gauge dynamometer. After drilling, hole quality evaluation has been processed on a non-contact video measuring system (VMS). The CFRP sample delamination (F_d) and an overcut (OC) were evaluated by applying Eqs. (1) and (2), respectively:

$$F_d = \frac{D_{max}}{D} \tag{1}$$

where D_{max} is the maximum damaged diameter (mm) and D is the drill diameter (mm).

$$OC = \frac{d_o - d_t}{2} \tag{2}$$

In this connection, d_o is the diameter of hole (mm) and d_t is the diameter of the tool (mm).

3 Results and Discussion

3.1 Thrust Force

The significance of spindle speed and rate of feed on thrust force for three different micro- and macro-drill diameters is illustrated in Fig. 4. In Fig. 4a, it was noticed that thrust force decreases with the increase in spindle speed for selected tool diameter. The reason for the decrease in the thrust force during the increase in the spindle speed was due to the temperature effects on resin and carbon fiber. Also, in Fig. 4b, it was noticed from the results that thrust force raises with the increase in the rate of feed for the selected tool diameter. The reason for increased thrust force based on the rate of feed was owing to an increase in cutting depth per revolution and thus the elevated shear area. The reason for increased thrust force was owing to more impact on cutting edge of drill, and the thrust force increases based on the selected tool diameter. That is, the thrust force increases when the drill diameter increases (F_y of Ø 0.5-mm drill > F_y of Ø 0.4-mm drill > F_y of Ø 0.3-mm drill for micro-drill and F_y of Ø 3-mm drill > F_y of Ø 2-mm drill > F_y of Ø 1-mm drill for macro-drill). Therefore, it was noticed that the increase in drill diameter results in increased thrust force for macro- and micro-drill. Moreover, the material removal rate was more at a higher rate of feed which results in increased

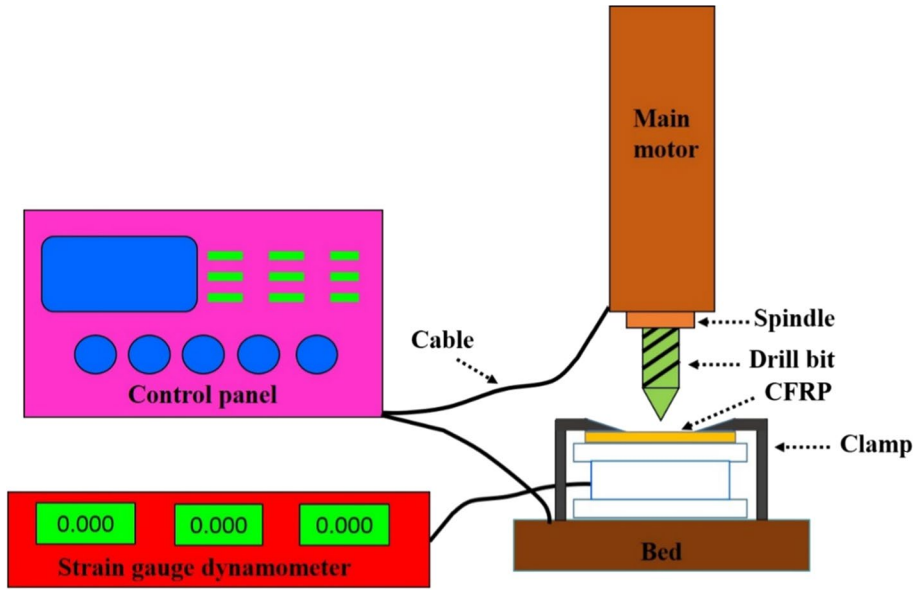

Fig. 2 Schematic representation of experimental setup utilized

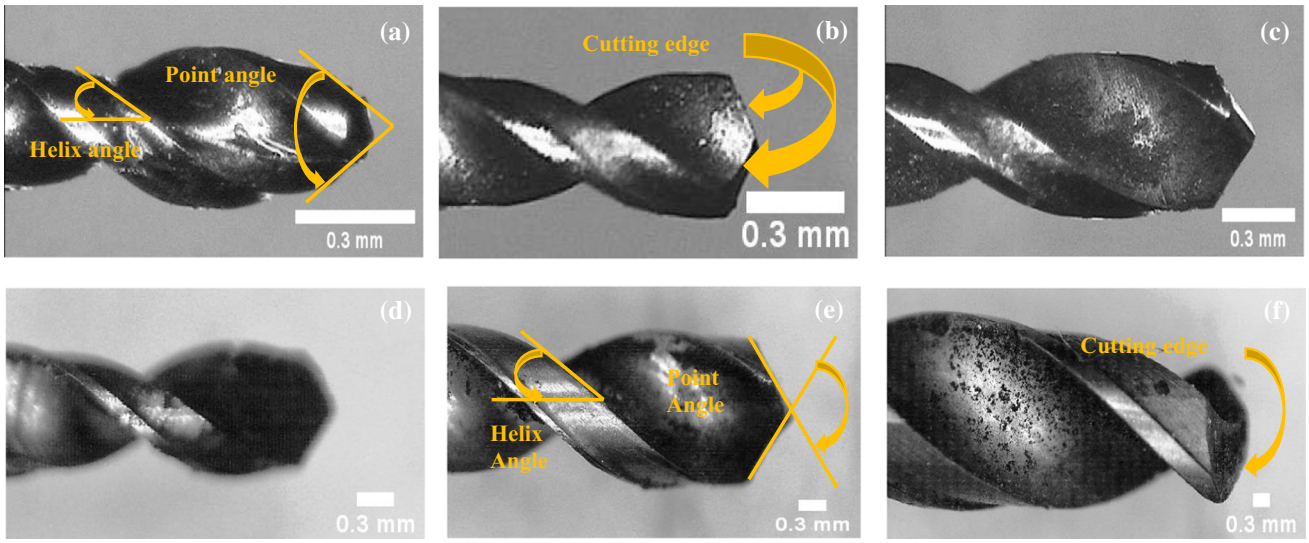

Fig. 3 Drill bit images before machining: micro-drill bits: **a** 0.3 mm, **b** 0.4 mm, **c** 0.5 mm and macro-drill bits: **d** 1 mm, **e** 2 mm and **f** 3 mm

Table 2 Specification of micro-drill and macro-drill

Drill diameter (mm)	0.3	0.4	0.5	1	2	3
Drill name	Multifaceted drill	Twist drill	Twist drill	Twist drill	Twist drill	Multifaceted drill
Drill materials	Carbide	Carbide	Carbide	Carbide	Carbide	Carbide
Shank type	Cylindrical	Cylindrical	Cylindrical	Cylindrical	Cylindrical	Cylindrical
Number of flutes	2	2	2	2	2	2
Point angle (°)	64	128	101	166	130	109
Helix angle (°)	28	26	27	30	43	40
Total length (mm)	38	38	38	38	38	38

Table 3 Measured responses for micro- and macro-drilling

Runs	*V*	*F*	Thrust force (N)			Delamination			Overcut (mm)		
			Drill diameter (mm)			Drill diameter (mm)			Drill diameter (mm)		
			0.3	0.4	0.5	0.3	0.4	0.5	0.3	0.4	0.5
Micro-drill											
1	2000	0.01	0.98	1.52	1.92	1.058	1.035	1.019	0.027	0.032	0.037
2	2000	0.03	1.52	1.92	2.36	1.084	1.076	1.060	0.022	0.023	0.025
3	2000	0.05	1.89	2.16	2.54	1.094	1.085	1.069	0.014	0.016	0.018
4	2500	0.01	0.96	1.50	1.91	1.064	1.036	1.020	0.028	0.033	0.036
5	2500	0.03	1.49	1.84	2.35	1.089	1.078	1.062	0.023	0.025	0.024
6	2500	0.05	1.85	2.03	2.49	1.099	1.086	1.068	0.016	0.017	0.019
7	3000	0.01	0.94	1.48	1.89	1.069	1.037	1.021	0.031	0.034	0.035
8	3000	0.03	1.45	1.82	2.26	1.092	1.089	1.073	0.026	0.028	0.029
9	3000	0.05	1.78	2.01	2.41	1.101	1.108	1.070	0.017	0.018	0.020
Runs	*V*	*F*	Thrust force (N)			Delamination			Overcut (mm)		
			Drill diameter (mm)			Drill diameter (mm)			Drill diameter (mm)		
			1	2	3	1	2	3	1	2	3
Macro-drill											
1	2000	0.01	2.35	2.65	2.99	1.045	1.026	1.010	0.034	0.036	0.041
2	2000	0.03	2.85	3.14	3.36	1.073	1.064	1.050	0.026	0.028	0.038
3	2000	0.05	2.92	3.26	3.54	1.081	1.073	1.058	0.019	0.021	0.024
4	2500	0.01	2.34	2.62	2.98	1.051	1.025	1.011	0.036	0.038	0.042
5	2500	0.03	2.84	3.11	3.35	1.076	1.065	1.051	0.026	0.029	0.033
6	2500	0.05	2.82	3.12	3.49	1.084	1.072	1.057	0.021	0.025	0.026
7	3000	0.01	2.36	2.67	2.98	1.057	1.025	1.012	0.037	0.039	0.041
8	3000	0.03	2.78	3.09	3.34	1.085	1.074	1.062	0.026	0.031	0.036
9	3000	0.05	2.80	3.11	3.41	1.092	1.095	1.058	0.025	0.027	0.028

thrust force. Among the various micro-drills, 0.3-mm drill produced lesser thrust force in the range of 0.96–1.84 N and 3-mm drill produced higher thrust force in the range of 2.98–3.48 N. The reason for the lesser thrust force in 0.3-mm drill was the lower shear area [17]. Also, the induced thrust force was indirectly proportional to the drill diameter and directly proportional to the rate of feed. In addition, the following formula was used to find the thrust force reduction percentage which is expressed in Eq. (3).

$$\text{Thrust force reduction \%} = \frac{(\text{high drill diameter} - \text{small drill diameter})}{\text{high drill diameter}} \times 100 \quad (3)$$

The thrust force reduction (36%) was observed between 0.3-mm drill and 0.4-mm drill combination which is less compared to 0.4-mm drill and 0.5-mm drill combination using the rate of feed of 0.01 mm/rev. The thrust force reduction (11.285%) was observed between 2-mm drill and 3-mm drill combination which is less compared to 1-mm drill and 2-mm drill combination using the feed of 0.01 mm/rev. Normally, the twist drill with low point angle produced lesser thrust force in the FRP drilling. The present results of 0.3-mm drill with 64° point angle produced lesser thrust force. Therefore, the point angle was affecting the induced thrust force for 0.3-mm drill because of interlaminar fracture toughness, Poisson's ratio, and Young's modulus of material.

3.2 Delamination Factor

The significance of spindle speed and rate of feed on the delamination factor for various micro- and macro-drill diameters is illustrated in Fig. 5. In Fig. 5a, it was noticed that delamination increases with the increase in spindle speed for selected tool diameter. Also, in Fig. 5b, as the rate of feed increases, delamination also increases for all the diameters. The low spindle speed and rate of feed produced minimum delamination owing to the heating of epoxy resin. Also, the minimum delamination effect was involved to reduce the stiffness of machined work material. Throughout the depth of the hole, the minimum delaminations were also observed in the inner circumferences hole. The delamination

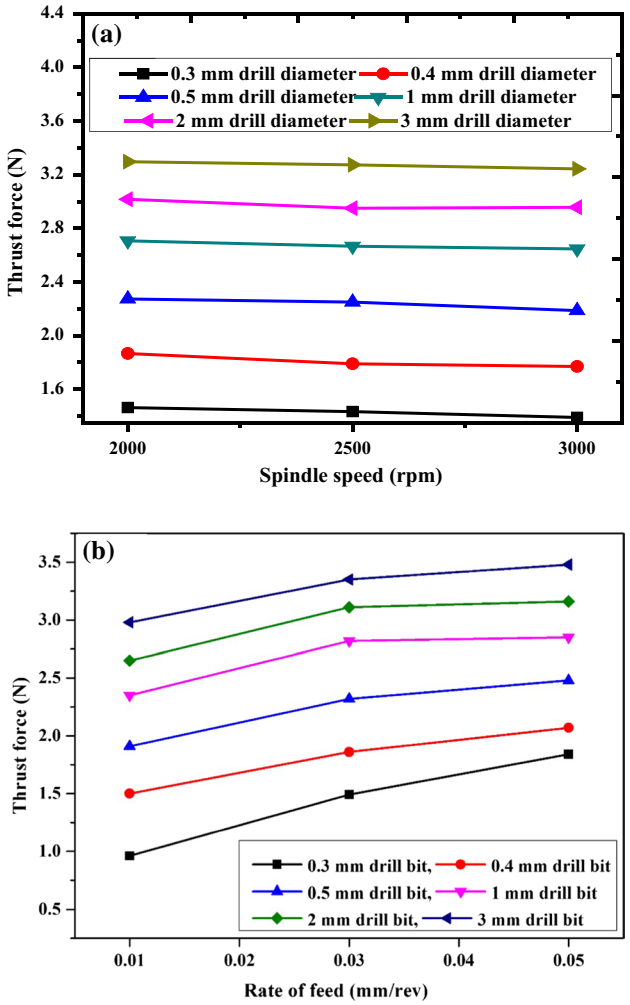

Fig. 4 Thrust force analysis based on **a** spindle speed, **b** rate of feed

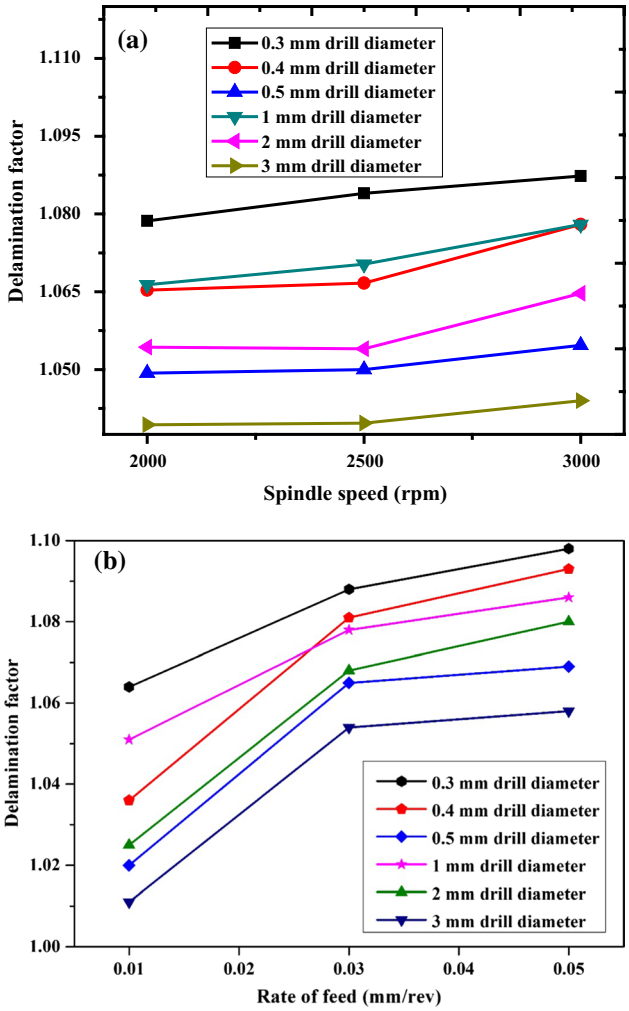

Fig. 5 Delamination factor analysis based on **a** spindle speed, **b** rate of feed

was increasing with the increase in the rate of feed, and various thrust forces were observed with the increase in the rate of feed. The reason for increasing the delamination was because a higher rate of feed produced higher thrust force. Therefore, more delamination was observed by using a higher rate of feed. Among the different micro-drills, a 0.3-mm drill produced maximum delamination on the CFRP in the range of 1.064–1.098. The induced delamination was reduced by changing drill diameter from 0.4 to 0.5 mm and a changing point angle from 128° to 101°. But, the drill diameter of 0.3 mm produced greater delamination than 0.4-mm drill (1.036–1.093) and 0.5-mm drill (1.020–1.069). Normally, the drill diameter increases with an increase in delamination because the higher contact area of drill produced higher delamination. But, the current results were reversely observed. This may be due to the measurement differences and tool geometrical differences. Hence, the delamination range is calculated by the difference between the maximum delamination and minimum delamination of each drill diameter. The delamination of 0.3-mm drill, 0.4-mm drill, and 0.5-mm drill was found to be 0.034, 0.057, and 0.049, respectively. The delamination range differences were observed in the micron levels. Similarly, in macro-drill, a 1-mm drill produced delamination in the range of 1.051–1.086. The induced delamination was reduced by changing drill diameter from 1 to 3 mm and a changing point angle from 166° to 109°. But, the 1-mm drill provided higher delamination than a 2-mm drill (1.025–1.080) and a 3-mm drill (1.011–1.058). Similar results were observed in the micro-drill. The 0.5-mm drill and 3-mm drill produced minimum delamination in the range of 1.02–1.069 and 1.011–1.058, respectively. This may be due to the increases in solid carbide drill size; the thermal stability and hot hardness of solid carbide drill also increased simultaneously [18]. Finally, the delamination was indirectly proportional to the drill diameter and directly proportional to the rate of

feed. In addition, the delamination reduction percentage is calculated by using Eq. (4).

$$\text{Delamination reduction \%} = \frac{(\text{small drill diameter} - \text{high drill diameter})}{\text{small drill diameter}} \times 100 \quad (4)$$

The delamination reduction (2.601%) was observed between 0.3-mm drill and 0.4-mm drill combination which is a higher reduction compared to 0.4-mm drill and 0.5-mm drill combination using the rate of feed of 0.01 mm/rev. The delamination reduction (2.442%) was observed between the 1-mm drill and 2-mm drill combination which is a higher reduction compared to 2-mm drill and 3-mm drill combination using the rate of feed of 0.01 mm/rev. The fiber interface bonding and fiber orientation were the major reason in variations of delamination reduction [19].

3.3 Overcut

The effect of spindle speed and rate of feed on overcut for the various macro- and micro-drills is presented in Fig. 6. In Fig. 6a, it was noticed that overcut increases with the increase in spindle speed for selected tool diameter. The reason for the increased overcut was the vibration of the drill bit based on the increase in spindle speed. Also, in Fig. 6b, it was noticed that overcut decreases with the increase in the rate of feed for selected tool diameter. That is, by changing the drill diameter from 3 mm to 1 mm and 0.5 mm to 0.3 mm, overcut decreased in the range from 0.041 to 0.026 mm and 0.028 to 0.015 mm, respectively. This was due to the higher rate of feed that increases the penetration rate which led to a decrease in machining time. So, decreases in machining time result in an overcut reduction. During CFRP drilling, an increase in temperature is due to frictional heating and results in variation in drill diameters. The overcut of 0.3-mm drill was lower than 0.4- and 0.5-mm drill as shown in Fig. 6. Similarly, overcut of 1-mm drill was lower than 2- and 3-mm drill. While comparing the performance of all the selected ranges of diameter, minimum overcut was obtained for 0.3-mm micro-drill and 1-mm macro-drill. In another word, overcut was defined by obtained variations in hole diameter. Hence, 0.3- and 1-mm drills provide minimum overcut due to less thrust force generation. The 0.5- and 3-mm drills provided the maximum overcut due to the higher thrust force generation. In addition, obtained hole diameter has a minimum deviation at a high rate of feed and maximum deviation at the low rate of feed. Finally, the overcut was indirectly proportional to the drill diameter and rate

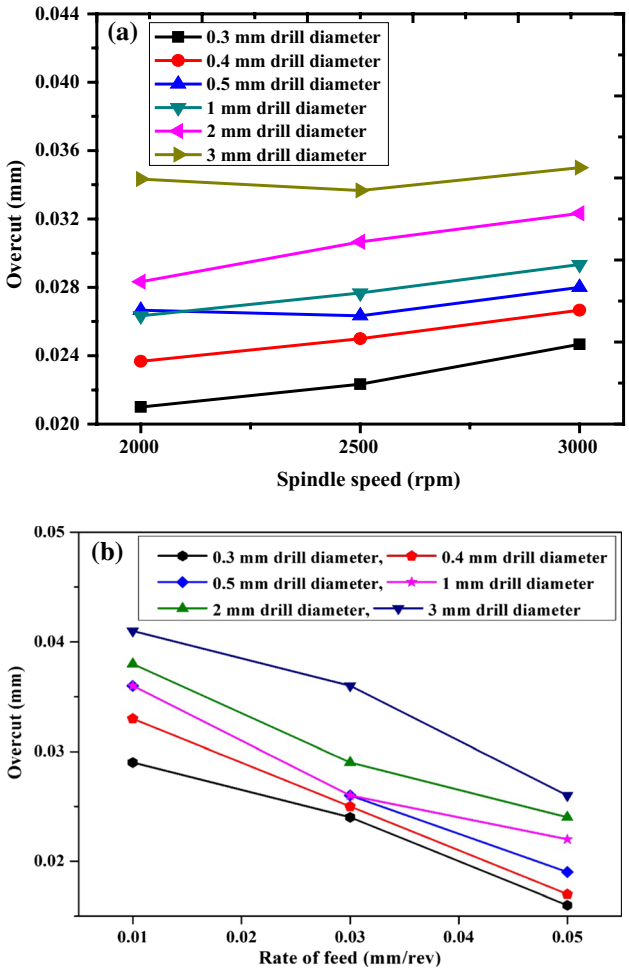

Fig. 6 Overcut analysis based on **a** spindle speed, **b** rate of feed

of feed. In addition, the overcut reduction percentage is expressed in Eq. (5).

$$\text{Overcut reduction \%} = \frac{(\text{high drill diameter} - \text{small drill diameter})}{\text{high drill diameter}} \times 100 \quad (5)$$

The overcut reduction (13.131%) was observed between 0.3-mm drill and 0.4-mm drill combination which is less compared to 0.4-mm drill and 0.5-mm drill combination using the rate of feed of 0.01 mm/rev. The overcut reduction (17.757%) was observed between 2-mm drill and 3-mm drill combination which is less compared to 1-mm drill and 2-mm drill combination using the rate of feed of 0.03 mm/rev. The minimum overcut was achieved by using a lower drill diameter with a lower point angle due to the geometrical differences.

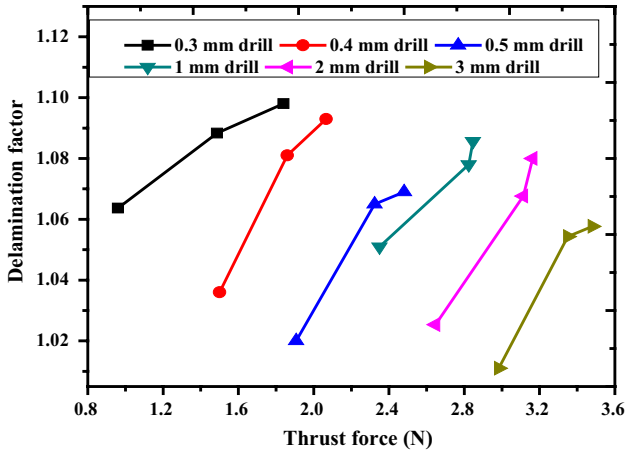

Fig. 7 Thrust force against delamination

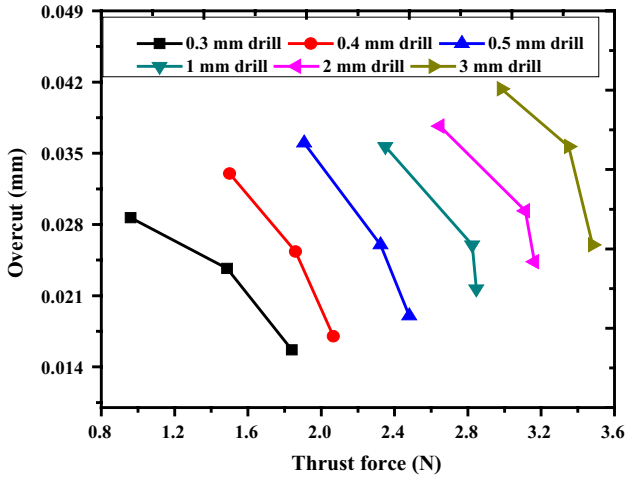

Fig. 8 Thrust force against overcut

3.4 Influence of Thrust Force on Delamination and Overcut

Figures 7 and 8 show the graph of thrust force on delamination and overcut, respectively, for all six drills. It can be noticed that thrust force increases and delamination also increases for all the six drills. The induced thrust force of 0.3-mm drill increased from 0.96 to 1.84 N as shown in Fig. 7. Therefore, a 0.3-mm drill produced maximum delamination among the remaining drill diameter. Similarly, the induced thrust force increased when the drill diameter increases. Therefore, it can be identified that the minimum induced thrust force of all the drill diameter was observed at minimum delamination factor. Among three different micro-drills, a 0.5-mm drill provided a 1.91 N thrust force with the least delamination factor (1.02). Similarly, a 3-mm drill provided 2.98 N thrust force with the least delamination factor (1.011). Velayudham and Krishnamurthy [20] found that the thrust force increased from 120 to 390 N with the increases in delamination. The thrust force increased from 40 N to 80 N with the increases in delamination from 1.0 to 1.11 for tripod drilling and 1.21–1.23 for WT drill of polymeric composites. The minimum delamination was found with a higher diameter of drill and a lower rate of feed. The supportive result found that the linear fitting curve was observed between the thrust force and the delamination factor [21]. In Fig. 8, it can be noticed that there is an increase in thrust force and a decrease in overcut for all the six drills. The induced thrust force of 0.3-mm drill diameter was ranging from 0.96 to 1.84 N, and it is shown in Fig. 8. Therefore, a 0.3-mm drill produced minimum overcut among the remaining drill diameters. Similarly, the induced overcut increased when the drill diameter increases. The overcut ratio increased from minimum to maximum while increasing the drill diameter in the order of 0.3-mm, 0.4-mm, 0.5-mm, 1-mm, 2-mm, and 3-mm drill.

Among various micro-drills, 0.3-mm drill provided a 1.84 N thrust force with maximum delamination (1.098) and minimum overcut (0.016 mm). Similarly, among various macro-drills, a 1-mm drill provided a 2.98 N thrust force with maximum delamination (1.086) and minimum overcut (0.022 mm). The minimum overcut was observed in the lower diameter, and a higher rate of feed was preferred in this condition. The maximum overcut was observed in the lower rate of feed because unwanted lateral vibrations of all drills also increase [22].

3.5 Analysis of Variables

The significance of input process variables was determined using ANOVA as shown in Tables 4, 5, 6, 7, 8, and 9. The rate of feed has a significant effect on F_y, F_d, and overcut. Based on the 'P' value, the rate of feed was identified as the significant process variable for all the micro- and macro-drills.

3.6 Optimum Analysis

In order to enhance the production quality, multiple quality characteristics are considered and gray relational theory was employed. In normalization of desired quality characteristics, thrust force, delamination, and overcut were considered as lower the better. The weightage of thrust force, delamination, and overcut was 0.5%, 0.25%, and 0.25%, respectively. The reason for more weightage was considered to thrust force due to tool geometry. It creates more problem on hole quality, and the tool diameter is directly proportional to thrust force. Therefore, 0.5% weightage was assigned to thrust force and 0.25% weightage was assigned to both delamination and overcut. In GRA, the observed results are normalized to the limit of 0–1 and gray coefficients

Table 4 Analysis of variance—0.3-mm drill

Thrust force						
S	DF	Seq-SS	Adj-SS	Adj-MS	*F*	*P*
V	2	0.0081	0.0081	0.00408	12.4	0.019
F	2	1.1766	1.1766	0.58831	1794.8	0
E	4	0.0013	0.0013	0.00033		
T	8	1.1860				
S = 0.0181046 *R*-Sq = 99.89% *R*-Sq(adj) = 99.78%						
Delamination @ entry						
V	2	0.0001	0.0001	5.73E−05	49	0.002
F	2	0.0018	0.00188	0.00094	806	0
E	4	4.7E−06	4.7E−06	1.2E−06		
T	8	0.001				
S = 0.00108012 *R*-Sq = 99.8% *R*-Sq-(adj) = 99.5%						
Overcut @ entry						
V	2	2E−05	2E−05	1E−05	31.1	0.004
F	2	0.0002	0.00025	0.000129	387	0
E	4	1.3E−06	1E−06	3E−07		
T	8	0.0003				
S = 0.000577350 *R*-Sq = 99.52% *R*-Sq(adj) = 99.05%						

S—source, *V*—spindle speed, *F*—rate of feed, *E*—error, *T*—total, DF—degree of freedom

Table 5 Analysis of variance—0.4-mm drill

Thrust force						
S	DF	Seq-SS	Adj-SS	Adj-MS	*F*	*P*
V	2	0.0156	0.0156	0.00781	7.73	0.042
F	2	0.4934	0.4934	0.24671	244	0
E	4	0.0040	0.0040	0.00101		
T	8	0.5130				
S = 0.0317980 *R*-Sq = 99.21% *R*-Sq(adj) = 98.42%						
Delamination @ entry						
V	2	0.00029	0.000290	0.000145	3.95	0.113
F	2	0.00541	0.00541	0.002709	73.55	0.001
E	4	0.0001	0.000147	3.68E−05		
T	8	0.0058				
S = 0.00606905 *R*-Sq = 97.5% *R*-Sq-(adj) = 95%						
Overcut @ entry						
V	2	1.36E−05	0.000013	6.8E−06	8.71	0.035
F	2	0.00038	0.000384	0.000192	247	0
E	4	3.1E−06	0.000003	8E−07		
T	8	0.00040				
S = 0.000881917 *R*-Sq = 99% *R*-Sq-(adj) = 98%						

were developed to represent the relation between ideal and observed values. The gray relational grade values are estimated by taking the average of GRC values. The highest GRG with the corresponding factor combination indicates the optimal setting. Tables 10 and 11 show the evaluated GRG for micro-drill and macro-drill. The 0.3-, 0.4-, 0.5-, 1-, and 3-mm drills achieved the highest GRG with the corresponding optimum factors in experimental number one. The 2-mm drill achieved the highest GRG with the corresponding optimum factors in experimental number four. Among the micro- and macro-drills, the best-obtained hole was evaluated based on the GRG value. Therefore, 0.3-mm and 2-mm drills make the best hole among the three different micro- and macro-drills, respectively. Confirmation tests were performed for 0.3-mm and 2-mm drills with the corresponding optimum setting on CFRP. The confirmation

Table 6 Analysis of variance—0.5-mm drill

Thrust force						
S	DF	Seq-SS	Adj-SS	Adj-MS	*F*	*P*
V	2	0.0120	0.0120	0.0060	7.87	0.041
F	2	0.5268	0.5268	0.2634	343.61	0
E	4	0.0030	0.0030	0.0007		
T	8	0.542				
S = 0.0276887 *R*-Sq = 99% *R*-Sq-(adj) = 99%						
Delamination @ entry						
V	2	5.07E−05	5.07E−05	2.53E−05	1.97	0.253
F	2	0.00444	0.00444	0.00222	173.06	0
E	4	5.13E−05	5E−05	1.28E−05		
T	8	0.0045				
S = 0.00358236 *R*-Sq = 99% *R*-Sq-(adj) = 98%						
Overcut @ entry						
V	2	4.7E−06	4.7E−06	2.3E−06	0.7	0.549
F	2	0.00043	0.00043	0.00021	65.7	0.001
E	4	1E−05	1E−05	3E−06		
T	8	0.00045				
S = 0.00182574 *R*-Sq = 97.08% *R*-Sq(adj) = 94.15%						

Table 7 Analysis of variance—1 mm drill

Thrust force						
S	DF	Seq-SS	Adj-SS	Adj-MS	*F*	*P*
V	2	0.0056	0.005	0.002	1.95	0.25
F	2	0.4712	0.4712	0.2356	164.4	0
E	4	0.0057	0.00573	0.0014		
T	8	0.482				
S = 0.0378594 *R*-Sq = 98.81% *R*-Sq(adj) = 97.62%						
Delamination @ entry						
V	2	0.00021	0.00021	0.00010	111.65	0
F	2	0.0019	0.00199	0.00099	1053.29	0
E	4	3.8E−06	3.8E−06	9E−07		
T	8	0.00220				
S = 0.000971825 *R*-Sq = 99.83% *R*-Sq(adj) = 99.66%						
Overcut @ entry						
V	2	1.36E−05	1.36E−05	6.8E−06	2.77	0.16
F	2	0.00030	0.00030	0.00015	63.05	0.001
E	4	9.8E−06	9.8E−06	2.4E−06		
T	8	0.000332				
S = 0.00156347 *R*-Sq = 97.05% *R*-Sq(adj) = 94.10%						

results are shown in Tables 12 and 13. The optimized parameters show a significant improvement in performance.

In the initial condition, to position the drill bit on the desired point of CFRP was a little difficult. However, the drill bit was positioned on the desired point with micron-level deviation. The produced micro-holes on the CFRP were not properly identified either it's through or blind hole. Figure 9 shows the picture of produced micro-hole on CFRP. During the machining time, carbon fiber and resins were sticking on drill flute as shown in Fig. 10. This may affect drill functionality and hole accuracy. Besides, the collected powders were showing the carbon fiber with resins as shown in Fig. 11. The reason for discontinuous chip and powder form of CFRP produced in the machining was the brittleness of materials and brittle fracture mechanism. The tool wears were not observed in all the drills because of the less material thickness and a number of

Table 8 Analysis of variance—2-mm drill

Thrust force						
S	DF	Seq-SS	Adj-SS	Adj-MS	*F*	*P*
V	2	0.0080	0.0080	0.0040	1.9	0.263
F	2	0.4872	0.4872	0.2436	114.49	0
E	4	0.0085	0.0085	0.0021		
T	8	0.5038				
S = 0.0461278 *R*-Sq = 98.31% *R*-Sq(adj) = 96.62%						
Delamination @ entry						
V	2	0.00022	0.00022	0.0001	2.47	0.2
F	2	0.00493	0.00493	0.00246	55.22	0.001
E	4	0.00017	0.00017	4.47E−05		
T	8	0.00533				
S = 0.00668331 *R*-Sq = 96.65% *R*-Sq(adj) = 93.30%						
Overcut @ entry						
V	2	2.42E−05	2.42E−05	1.21E−05	12.82	0.018
F	2	0.00027	0.00027	0.00013	144.12	0
E	4	3.8E−06	3.8E−06	9E−07		
T	8	0.0003				
S = 0.000971825 *R*-Sq = 98.74% *R*-Sq(adj) = 97.48%						

Table 9 Analysis of variance—3 mm drill

Thrust force						
S	DF	Seq-SS	Adj-SS	Adj-MS	*F*	*P*
A	2	0.0042	0.0042	0.0021	1.87	0.26
B	2	0.3980	0.3980	0.1990	173.89	0
E	4	0.0045	0.0045	0.0011		
T	8	0.4068				
S = 0.0338296 *R*-Sq = 98.87% *R*-Sq(adj) = 97.75%						
Delamination @ entry						
A	2	4.07E−05	4.07E−05	2.03E−05	1.61	0.30
B	2	0.004067	0.00406	0.00203	160.53	0
E	4	5.07E−05	5.07E−05	1.27E−05		
T	8	0.004158				
S = 0.00355903 *R*-Sq = 98.78% *R*-Sq(adj) = 97.56%						
Overcut @ entry						
A	2	2.71E−06	2.71E−06	1.31E−06	0.29	0.76
B	2	0.000361	0.00036	0.0001	38.64	0.00
E	4	1.87E−05	1.87E−05	4.7E−06		
T	8	0.000382				
S = 0.00216025 *R*-Sq = 95.11% *R*-Sq(adj) = 90.23%						

experiments. The non-contact roughness measurement was used to measure the surface roughness of 0.5-mm micro-hole. Figure 12 shows the roughness of 1.48 µm for a 0.3-mm drilled hole. Figure 13a–f shows the microstructural defects of produced holes which are fiber overcut, fiber pull-in, fiber pull-in at the exit, resin melting, uneven hole rim at entry, uncut fiber, and long uncut fiber.

4 Conclusions

An experimental investigation was conducted for analyzing the micro-hole and macro-hole quality on CFRP. The relations between thrust force, delamination, and overcut for various drill diameters were analyzed. Taguchi-based gray relational analysis was followed to minimize the

Table 10 Evaluated gray relational grade for micro-drill

Run	Normalized values			Reference sequence			Gray relational coefficient			GRG	Rank
	F_y	F_d	OC	F_y	F_d	OC	F_y	F_d	OC		
0.3-mm drill											
1	0.96	1.000	0.235	0.04	0.000	0.765	0.92	1.000	0.246	0.723	1
2	0.39	0.395	0.529	0.61	0.605	0.471	0.45	0.293	0.347	0.363	7
3	0.00	0.163	1.000	1.00	0.837	0.000	0.33	0.230	1.000	0.521	4
4	0.98	0.860	0.176	0.02	0.140	0.824	0.96	0.642	0.233	0.611	2
5	0.42	0.279	0.471	0.58	0.721	0.529	0.46	0.257	0.321	0.347	8
6	0.04	0.047	0.882	0.96	0.953	0.118	0.34	0.208	0.680	0.410	5
7	1.00	0.744	0.000	0.00	0.256	1.000	1.00	0.494	0.200	0.565	3
8	0.46	0.209	0.294	0.54	0.791	0.706	0.48	0.240	0.262	0.328	9
9	0.12	0.000	0.824	0.88	1.000	0.176	0.36	0.200	0.586	0.382	6
0.4-mm drill											
1	0.94	1.00	0.11	0.06	0.000	0.889	0.89	1.000	0.220	0.705	1
2	0.35	0.44	0.61	0.65	0.562	0.389	0.44	0.308	0.391	0.378	7
3	0.00	0.32	1.00	1.00	0.685	0.000	0.33	0.267	1.000	0.534	4
4	0.97	0.99	0.06	0.03	0.014	0.944	0.94	0.948	0.209	0.701	2
5	0.47	0.41	0.50	0.53	0.589	0.500	0.49	0.298	0.333	0.372	8
6	0.19	0.30	0.94	0.81	0.699	0.056	0.38	0.264	0.818	0.488	5
7	1.00	0.97	0.00	0.00	0.027	1.000	1.00	0.901	0.200	0.700	3
8	0.50	0.26	0.33	0.50	0.740	0.667	0.50	0.253	0.273	0.342	9
9	0.22	0.00	0.89	0.78	1.000	0.111	0.39	0.200	0.692	0.428	6
0.5-mm drill											
1	0.95	1.000	0.000	0.05	0.000	1.000	0.92	1.000	0.200	0.705	1
2	0.28	0.241	0.632	0.72	0.759	0.368	0.41	0.248	0.404	0.354	8
3	0.00	0.074	1.000	1.00	0.926	0.000	0.33	0.213	1.000	0.515	4
4	0.97	0.981	0.053	0.03	0.019	0.947	0.94	0.931	0.209	0.694	3
5	0.29	0.204	0.684	0.71	0.796	0.316	0.41	0.239	0.442	0.365	7
6	0.08	0.093	0.947	0.92	0.907	0.053	0.35	0.216	0.826	0.464	5
7	1.00	0.963	0.105	0.00	0.037	0.895	1.00	0.871	0.218	0.696	2
8	0.43	0.000	0.421	0.57	1.000	0.579	0.47	0.200	0.302	0.323	9
9	0.20	0.056	0.895	0.80	0.944	0.105	0.38	0.209	0.704	0.433	6

experiment trails and find the optimum levels. The following conclusions were drawn based on the outcomes.

- From the analysis, micro- and macro-drills linearly affect the thrust force and delamination and are inversely proportional to overcut. A rapid decrease was observed on overcut for the rate of feed above 0.01 mm/rev.
- Among the micro-drill, a 0.3-mm drill produced the best hole at lower levels of spindle speed and rate of feed. Similarly, a 2-mm macro-drill produced the best hole at medium spindle speed and a lower rate of feed. The measured surface roughness on the drilled hole was found as a minimum.
- From the statistical analysis, the rate of feed was identified as a major process variable which influences the desired performance measures such as thrust force, delamination, and overcut for all the selected ranges of micro- and macro-drill parameters.
- The proposed Taguchi-based gray relational approach enhances the multi-performance drilling characteristics for the micro- and macro-drilling processes.
- The micro-drilling performance could be analyzed using a laser processing method and abrasive water jet machining in the future.

Table 11 Evaluated gray relational grade for macro-drill

–	Normalized values			Reference sequence			Gray relational coefficient			GRG	Rank
	F_y	F_d	OC	F_y	F_d	OC	F_y	F_d	OC		
1-mm drill											
1	0.98	1.000	0.167	0.02	0.000	0.833	0.97	1.000	0.231	0.732	1
2	0.12	0.404	0.611	0.88	0.596	0.389	0.36	0.296	0.391	0.350	6
3	0.00	0.234	1.000	1.00	0.766	0.000	0.33	0.246	1.000	0.526	4
4	1.00	0.872	0.056	0.00	0.128	0.944	1.00	0.662	0.209	0.624	2
5	0.14	0.340	0.611	0.86	0.660	0.389	0.37	0.275	0.391	0.344	7
6	0.17	0.170	0.889	0.83	0.830	0.111	0.38	0.232	0.692	0.433	5
7	0.97	0.745	0.000	0.03	0.255	1.000	0.94	0.495	0.200	0.543	3
8	0.24	0.149	0.611	0.76	0.851	0.389	0.40	0.227	0.391	0.339	8
9	0.21	0.000	0.667	0.79	1.000	0.333	0.39	0.200	0.429	0.338	9
2-mm drill											
1	0.95	0.986	0.167	0.05	0.014	0.833	0.91	0.946	0.231	0.697	2
2	0.19	0.443	0.611	0.81	0.557	0.389	0.38	0.310	0.391	0.361	6
3	0.00	0.314	1.000	1.00	0.686	0.000	0.33	0.267	1.000	0.534	4
4	1.00	1.000	0.056	0.00	0.000	0.944	1.00	1.000	0.209	0.736	1
5	0.23	0.429	0.556	0.77	0.571	0.444	0.40	0.304	0.360	0.353	7
6	0.22	0.329	0.778	0.78	0.671	0.222	0.39	0.271	0.529	0.397	5
7	0.92	1.000	0.000	0.08	0.000	1.000	0.86	1.000	0.200	0.688	3
8	0.27	0.300	0.444	0.73	0.700	0.556	0.41	0.263	0.310	0.326	9
9	0.23	0.000	0.667	0.77	1.000	0.333	0.40	0.200	0.429	0.341	8
3-mm drill											
1	0.98	1.000	0.056	0.02	0.000	0.944	0.97	1.000	0.209	0.725	1
2	0.32	0.231	0.222	0.68	0.769	0.778	0.42	0.245	0.243	0.304	8
3	0.00	0.077	1.000	1.00	0.923	0.000	0.33	0.213	1.000	0.515	4
4	1.00	0.981	0.000	0.00	0.019	1.000	1.00	0.929	0.200	0.710	2
5	0.34	0.212	0.500	0.66	0.788	0.500	0.43	0.241	0.333	0.335	7
6	0.09	0.096	0.889	0.91	0.904	0.111	0.35	0.217	0.692	0.421	5
7	1.00	0.962	0.056	0.00	0.038	0.944	1.00	0.867	0.209	0.692	3
8	0.36	0.000	0.333	0.64	1.000	0.667	0.44	0.200	0.273	0.303	9
9	0.23	0.077	0.778	0.77	0.923	0.222	0.39	0.213	0.529	0.379	6

Table 12 Confirmation test results for 0.3-mm drill

Setting level	Initial setting	Optimal process parameters	
		Prediction	Experiment
	V1F1	V1F1	V1F1
F_y	0.98		0.92
F_d	1.058		1.042
OC	0.027		0.024
GRG	0.723	0.697	0.766
Improvement in gray relational grade = 0.043			

Table 13 Confirmation test for 2-mm drill

Setting level	Initial setting	Optimal process parameters	
		Prediction	Experiment
	V1F1	V2F1	V2F1
F_y	2.65		2.51
F_d	1.026		1.020
OC	0.036		0.018
GRG	0.697	0.744	0.736
Improvement in gray relational grade = 0.039			

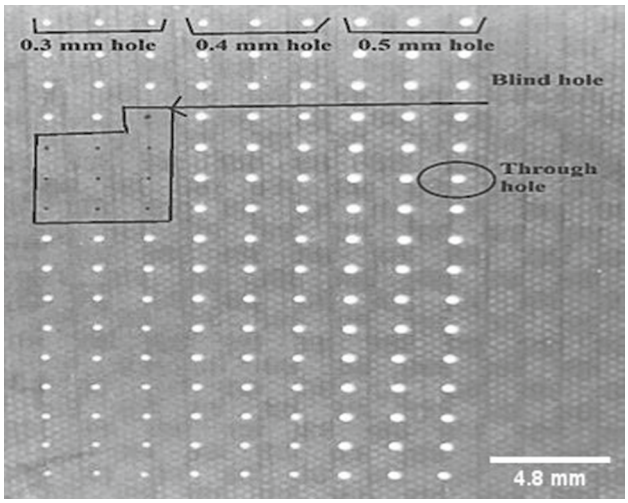

Fig. 9 Optical micrograph of micro-holed CFRP

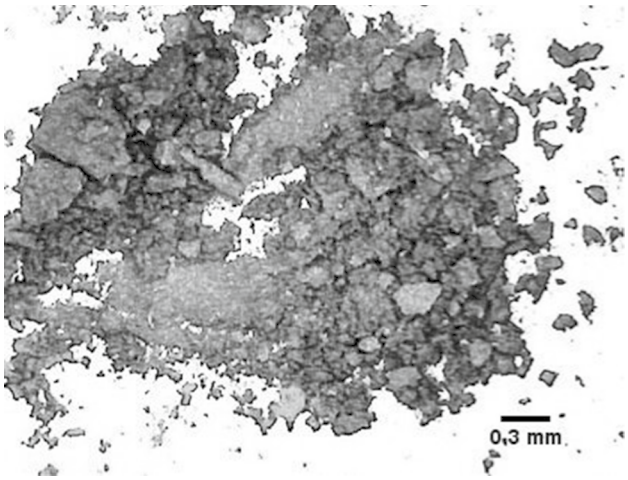

Fig. 11 Optical micrograph of sticking powder of carbon fiber with resin

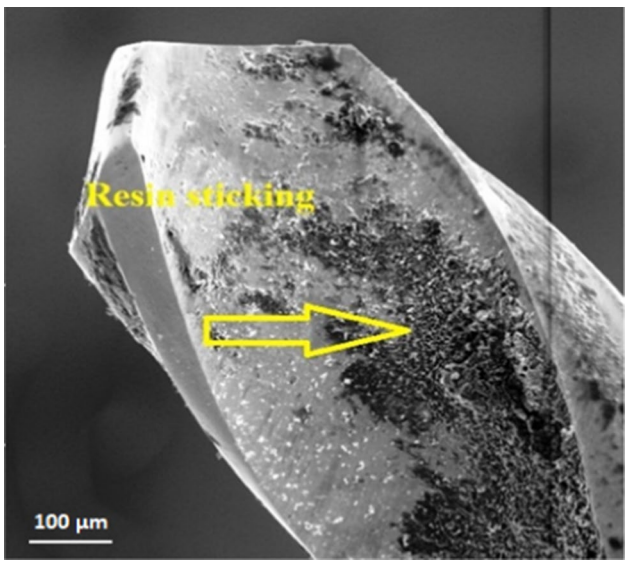

Fig. 10 SEM picture of sticking resin to 0.4-mm drill

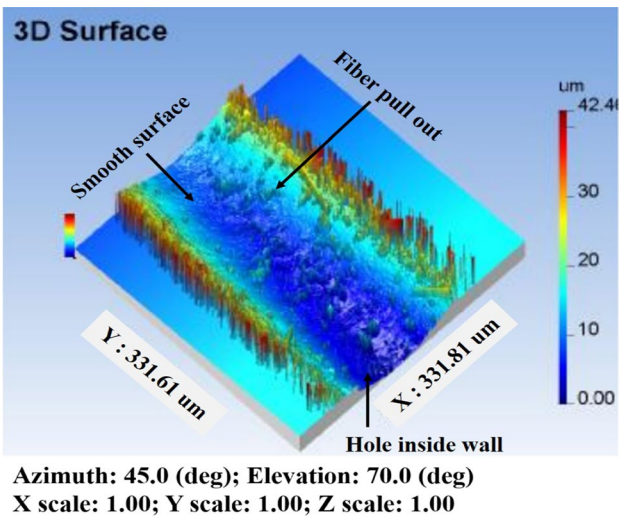

Fig. 12 Roughness inside the wall of 0.3-mm hole

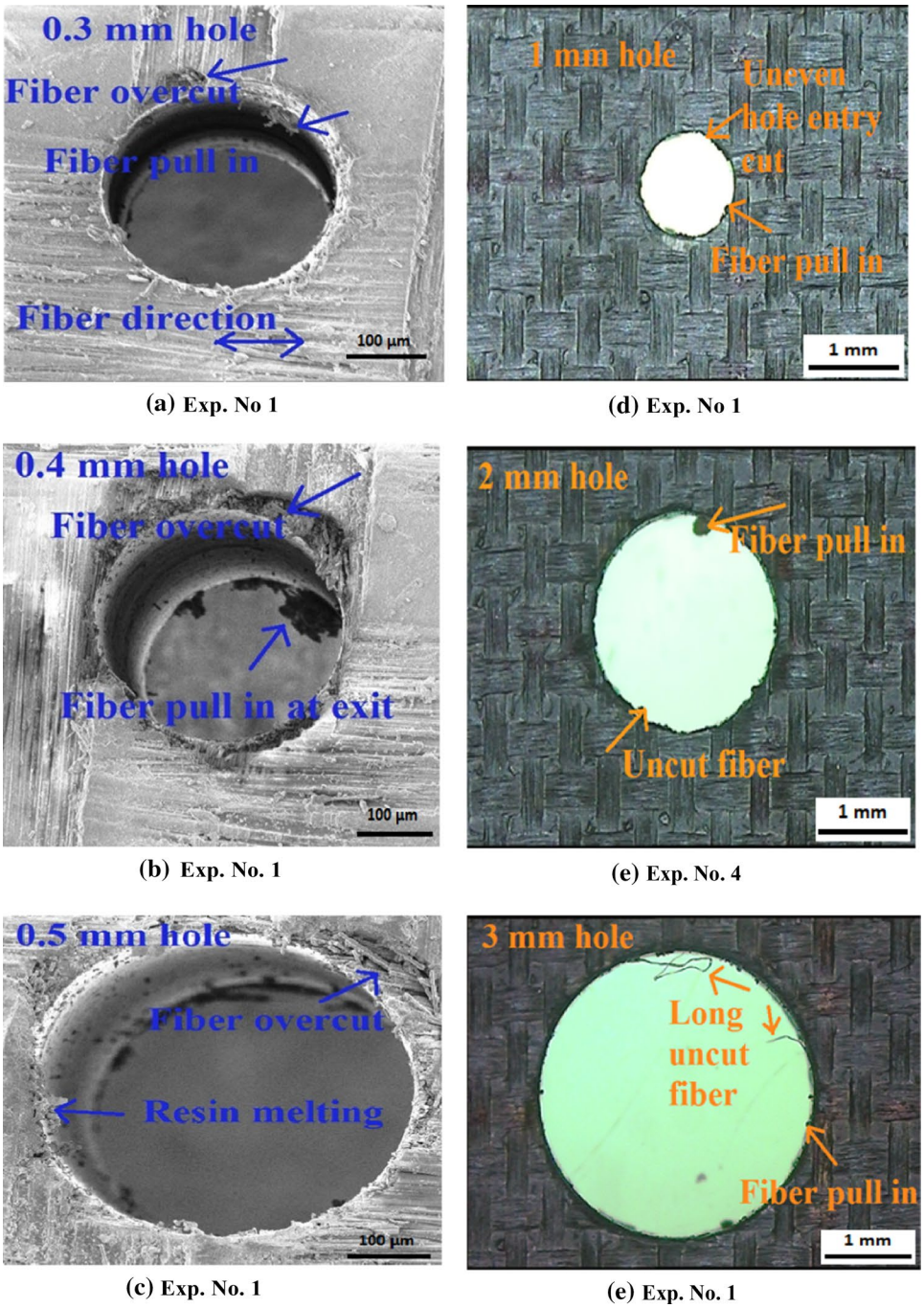

Fig. 13 Structure of holes **a** 0.3 mm [16], **b** 0.4 mm, **c** 0.5 mm, **d** 1 mm, **e** 2 mm, **f** 3 mm

Acknowledgements The authors wish to thank National Taipei University of Technology, Taipei-10608, Taiwan, ROC, Indian Institute of Technology Madras, India, and MAM School of Engineering, Tiruchirappalli, India, for all support required to carry out this research.

References

1. Raj, D.S.; Karunamoorthy, L.: Study of the effect of tool wear on hole quality in drilling CFRP to select a suitable drill for multi-criteria hole quality. Mater. Manuf. Process. **31**, 587–592 (2015). https://doi.org/10.1080/10426914.2015.1004713
2. Tan, C.L.; Azmi, A.I.; Muhammad, N.: Delamination and surface roughness analyses in drilling hybrid carbon/glass composite. Mater. Manuf. Process. **31**, 1366–1376 (2016). https://doi.org/10.1080/10426914.2015.1103864
3. Krishnaraj, V.; Prabukarthi, A.; Ramanathan, A.; Elanghovan, N.; Senthil Kumar, M.; Zitoune, R.; Davim, J.P.: Optimization of machining parameters at high speed drilling of carbon fiber reinforced plastic (CFRP) laminates. Compos. Part B Eng. **43**, 1791–1799 (2012). https://doi.org/10.1016/j.compositesb.2012.01.007

4. Eneyew, E.D.; Ramulu, M.: Experimental study of surface quality and damage when drilling unidirectional CFRP composites. J. Mater. Res. Technol. **3**, 354–362 (2014). https://doi.org/10.1016/j.jmrt.2014.10.003
5. Du, J.; Zhang, H.; Geng, Y.; Ming, W.; He, W.; Ma, J.; Cao, Y.; Li, X.; Liu, K.: A review on machining of carbon fiber reinforced ceramic matrix composites. Ceram. Int. **45**, 18155–18166 (2019). https://doi.org/10.1016/j.ceramint.2019.06.112
6. Daxi, G.; Yunda, T.; Yihang, L.; Zhenyu, S.; Xinggang, J.; Deyuan, Z.: Experimental study on drilling load and hole quality during rotary ultrasonic helical machining of small-diameter CFRP holes. J Mater. Process. Technol. **270**, 195–205 (2019). https://doi.org/10.1016/j.jmatprotec.2019.03.001
7. John, K.M.; Thirumalai Kumaran, S.; Rendi, K.; Park, Ki M.; Byeon, J.H.: Review on the methodologies adopted to minimize the material damages in drilling of carbon fiber reinforced plastic composites. J Reinf. Plast. Compos. **38**, 351–368 (2019). https://doi.org/10.1177/0731684418819822
8. Panchagnula, K.K.; Palaniyandi, K.: Drilling on fiber reinforced polymer/nanopolymer composite laminates: a review. J. Mater. Res. Technol. **7**, 180–189 (2018). https://doi.org/10.1016/j.jmrt.2017.06.003
9. Samuel Raj, D.; Karunamoorthy, L.: Performance of cryogenically treated WC drill using tool wear measurements on the cutting edge and hole surface topography when drilling CFRP. Int. J. Refract. Met. Hard Mater. **78**, 32–44 (2019). https://doi.org/10.1016/j.ijrmhm.2018.08.011
10. Mannoj Rajkumar, G.; Bhardwaj, D.; Kannan, C.; Oyyaravelu, R.; Balan, A.S.S.: Effect of chilled air on delamination, induced vibration, burr formation and surface roughness in CFRP drilling: a comparative study. Mater. Res. Express (2018). https://doi.org/10.1088/2053-1591/aaf47d
11. Durante, M.; Boccarusso, L.; De Fazio, D.; Langella, A.: Circular cutting strategy for drilling of carbon fiber-reinforced plastics (CFRPs). Mater. Manuf. Process. **34**, 554–5661 (2019). https://doi.org/10.1080/10426914.2019.1566615
12. Mudhukrishnan, M.; Hariharan, P.; Palanikumar, K.; Latha, B.: Optimization and sensitivity analysis of drilling parameters for sustainable machining of carbon fiber-reinforced polypropylene composites. J. Thermoplast. **32**, 1485–1508 (2018). https://doi.org/10.1177/0892705718799816
13. Qiu, X.; Li, P.; Niu, Q.; Chen, A.; Ouyang, P.; Li, C.; Jo, K.T.: Influence of machining parameters and tool structure on cutting force and hole wall damage in drilling CFRP with stepped drills. Int. J. Adv. Manuf. Technol. **97**, 857–865 (2018). https://doi.org/10.1007/s00170-018-1981-2
14. Zitoune, R.; Krishnaraj, V.; Collombet, F.: Study of drilling of composite material and aluminium stack. Compos. Struct. **92**, 1246–1255 (2010). https://doi.org/10.1016/j.compstruct.2009.10.010
15. Heisel, U.; Pfeifroth, T.: Influence of point angle on drill hole quality and machining forces when drilling CFRP. AIP Proc. CIRP **1**, 471–476 (2012). https://doi.org/10.1016/j.procir.2012.04.084
16. Raj Kumar, D.; Ranjithkumar, P.; Jenarthanan, M.P.; Sathiyanarayanan, C.: Experimental investigation and analysis of factors influencing delamination and thrust force during drilling of carbon-fibre reinforced polymer composites. Pigment Resin Technol. **46**(6), 507–524 (2017)
17. Karnik, S.R.; Gaitonde, V.N.; Rubio, J.C.; Correia, A.E.: Delamination analysis in high speed drilling of carbon fiber reinforced plastics (CFRP) using artificial neural network model. Mater. Des. **29**, 1768–1776 (2008). https://doi.org/10.1016/j.matdes.2008.03.014
18. Abish, J.; Samal, P.; Narenther, M.S.; Kannan, C.; Balan, A.S.S.: Assessment of drilling-induced damage in CFRP under chilled air environment. Mater. Manuf. Process. **33**, 1361–1368 (2018). https://doi.org/10.1080/10426914.2017.1415452
19. Ravi Shankar, A.; Karali, P.: Cutting force and hole quality analysis in micro-drilling of CFRP. Mater. Maunf. Process. **33**, 1369–1377 (2018). https://doi.org/10.1080/10426914.2017.1401715
20. Velayudham, A.; Krishnamurthy, R.: Effect of point geometry and their influence on thrust and delamination in drilling of polymeric composites. J. Mater. Process. Technol. **185**, 204–209 (2007). https://doi.org/10.1016/j.jmatprotec.2006.03.146
21. Liu, L.; Qi, C.; Wu, F.; Xu, J.; Zhu, X.: Experimental thrust forces and delamination analysis of GFRP laminates using candlestick drills. Mater. Manuf. Process. **33**, 695–708 (2018). https://doi.org/10.1080/10426914.2017.1376072
22. Anwar, S.; Nasr, M.M.; Pervaiz, S.; Al-Ahmari, A.; Alkahtani, M.; El-Tamimi, A.: A study on the effect of main process parameters of rotary ultrasonic machining for drilling BK7 glass. Adv. Mech. Eng. (2018). https://doi.org/10.1177/1687814017752212